J Low Temp Phys (2008) 151: 1080–1086
DOI 10.1007/s10909-008-9791-9

A Metallic Magnetic Calorimeter for Hard X-Ray and Gamma Ray Spectrometry

M. Rodrigues · E. Leblanc · M. Loidl · J. Bouchard · B. Censier · A. Fleischmann · A. Burck · H. Rotzinger · C. Enss

Received: 23 July 2007 / Accepted: 5 October 2007 / Published online: 22 February 2008

Abstract The CEA/LNHB is responsible for the determination and publication of atomic and nuclear data such as X-ray and gamma ray emission probabilities. In order to reduce uncertainties on the determination of these data, a high energy resolution associated with a good intrinsic detection efficiency is required. Hence taking into account these two aspects, we are developing cryogenic detectors, especially metallic magnetic calorimeters (MMCs) for photon spectrometry from few keV up to 200 keV.

A MMC using a meander pick-up coil made of niobium thin films has been optimized. The gold absorber (diameter: 1.1 mm, thickness: 335 μm) has an intrinsic detection efficiency larger than 70% for photons from few keV up to 100 keV. From an energy spectrum obtained with a ^{133}Ba multi-gamma source, we have characterized this first detector. The energy resolution is 320 eV and 560 eV respectively at 30 keV and 357 keV. Possible improvements of the performance of the detector are discussed.

PACS 29.30 Kv · 29.40.-n · 06.20.-f

1 Introduction

We are developing metallic magnetic calorimeters (MMCs) for metrology applications, especially for the determination of hard X-ray and γ-ray emission probabilities. A radioactive source containing one or several radionuclides, emits photons at different energies E with their associated emission probabilities $P(E)$. These probabilities

M. Rodrigues (✉) · E. Leblanc · M. Loidl · J. Bouchard · B. Censier
CEA/DRT/LIST/LNHB, Gif sur Yvette 91191, France
e-mail: matias_rodrigues80@hotmail.com

A. Fleischmann · A. Burck · H. Rotzinger · C. Enss
KIP, University of Heidelberg, Im Neuenheimer Feld 227, 69120 Heidelberg, Germany

are experimentally determined from an energy spectrum by the relation:

$$P(E) = \frac{N(E)}{A(t) \cdot \Delta t \cdot \Omega \cdot \varepsilon(E)}$$

where $N(E)$ is the number of detected events corresponding to the energy E, $A(t)$ is the source activity at the time t, $\varepsilon(E)$ is the intrinsic detection efficiency, Δt is the acquisition duration and Ω is the solid angle between the source and the detector.

Measurements of emission probabilities are commonly performed using germanium or silicon semiconductor detectors. Planar geometry detectors are used for the energy range of few hundred eV to 200 keV and coaxial geometry detectors for the energy range 50 keV to few MeV. The major part of the uncertainty related to $P(E)$ comes from the uncertainties on $\varepsilon(E)$ and $N(E)$. The uncertainty on $N(E)$ is due to the statistical uncertainty and the overlapping of the peaks corresponding to events of close energies, since the detector has a limited energy resolution $R(E)$.

In order to reduce the uncertainties caused by overlapping peaks we need to improve the energy resolution. However, the energy resolution of the semiconductors has reached its theoretical limit. Moreover, the presence of a dead layer and a window between the detector and the source require characterizing the energy dependence of detection efficiency with a large number of measurements and calibration sources [1]. MMCs can offer a high energy resolution associated with a good intrinsic detection efficiency [2] that should be easier to characterize (no dead layer or entrance window when the source is inside the cryostat). This is the reason why the LNHB is interested in the development of MMCs for the determination of emission probabilities.

2 Physics Principle

MMCs are thermal single-particle detectors. The detector is usually made of a gold absorber and a paramagnetic sensor which consists of gold doped with a few hundred ppm of erbium. The sensor is magnetized by an external magnetic field of a few mT. Below a temperature T of 100 mK, this magnetization is strongly dependent on the temperature.

The sensor is magnetically coupled to a DC SQUID magnetometer via a superconducting flux transformer consisting of a pick-up coil and an input coil. The interaction of a photon in the absorber leads to a temperature rise ΔT and a flux variation in the SQUID $\delta\Phi_s$ given by [3]:

$$\delta\Phi_S \propto \mu_0 V_{sensor} G \frac{\partial M}{\partial T} \frac{E_\gamma}{C_{sensor} + C_{abs}}$$

C_{sensor} and C_{abs} are respectively the heat capacities of the sensor and the absorber. M is the magnetization, V_{sensor} the sensor volume and G a coupling factor. The detector returns to its equilibrium temperature via a thermal link between the sensor and the thermal bath.

In order to have a high detection efficiency, a large absorber volume is required, i.e. a large sensor is needed (their both heat capacities have to be of the same order of

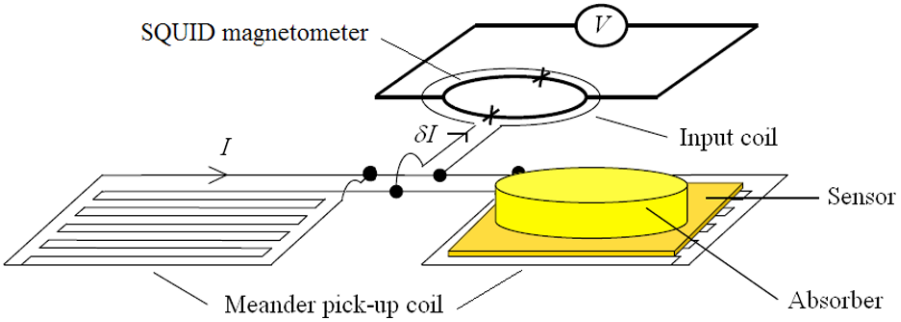

Fig. 1 (Color online) Scheme of the detector and the principle of the signal read-out

magnitude). In order to achieve an optimal coupling between the large sensor and the SQUID, a pick-up coil with a meander shape in thin film structure is used [4]. This pick-up coil is also used to magnetize the sensor by freezing a current I. Two pick-up coils are connected in parallel to avoid the current I to flow in the input coil (Fig. 1). The change of magnetization induces a change of current δI in the flux transformer and a flux variation $\delta\Phi_S$ through the SQUID.

3 Optimization

The meander pick-up coil geometry was optimized to maximize the signal to noise ratio under the assumption that the noise is dominated by the SQUID noise [3]. The meander has a surface of 1×1 mm^2.

In an independent way, the detector geometry was optimized taking into account the following constraints and choices. We want the best compromise between detection efficiency and energy resolution. The first parameter is the working temperature of our dilution cryostat which is about 20 mK. The second one is the minimal diameter of the absorber; it is set by the inner diameter of a tin collimator which has well characterized dimensions (inner diameter: 1 mm, thickness: 5 mm). The optimum thickness h_a of the gold absorber was selected by comparing the detection efficiency curves; they have been obtained by Monte Carlo simulation for different thicknesses and for photon energies up to 200 keV. In Fig. 2, one can notice for a thickness of about 330 μm, the intrinsic detection efficiency versus the photon energy is smoothed around the K-shell discontinuity (80.72 keV). The reason is that the detection efficiency just below and just above the K-shell discontinuity has not the same thickness dependence. The linear attenuation coefficient of gold just below the K-shell discontinuity is lower than the one just above, but above the K-shell discontinuity the detection efficiency is reduced by the X_K escape. A smoothed detection efficiency curve has the advantage to be easier to characterize.

Concerning the sensor geometry, its volume is given by its heat capacity. C_{sensor} was obtained by maximizing the calculated signal amplitude with the following parameters: a concentration of erbium of 900 ppm, a given absorber heat capacity C_a and the maximum current I frozen in the pick-up coil. This maximum current I

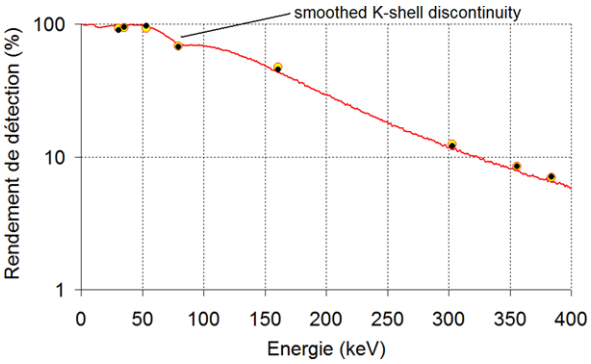

Fig. 2 (Color online) Comparison between the detection efficiency curves obtained by Monte Carlo simulation and experimental data. The *black dots* are experimental data, the *circles* are results from Monte Carlo simulations and the line is the results from Monte Carlo simulations with a simplified geometry

is estimated to be $I = 50$ mA for a pure and regular niobium thin film layer. The signal amplitude is maximized for a sensor heat capacity close to that of the absorber. The sensor surface is given by the pick-up coil size. The total heat capacity was determined by setting the theoretical energy resolution of the detector at 50 eV, taking into account the SQUID electronics noise, the magnetic Johnson noise and the fundamental limit of the energy resolution given by the thermodynamic fluctuations of energy [5]. This last constraint permits to fix the absorber diameter d_a and the sensor thickness h_s by numerical calculations: $d_a = 1.1$ mm, $h_s = 3.5$ µm and $C_{sensor} \sim C_{abs} = 5.10^{-10}$ J/K at 20 mK.

4 Experimental Set-up

The absorber of the detector has a diameter of 1.1 mm and a thickness of 335 µm. The thermal link is a gold ribbon wedge bonded on the sensor and the thermal bath. A simple way to characterize the detection efficiency as a function of energy is to measure a multi-gamma source. We have chosen ^{133}Ba which emits photons at several energies between 3.8 keV and 383.85 keV. The detector with the source and the collimator was installed in our dilution cryostat. The detector temperature has been regulated at 16 mK with a standard deviation of 2.4 µK. The detector is read-out by a two-stage SQUID set-up which permits to reduce the noise contribution of the room temperature electronics [6].

From a comparison of the measured and calculated dependence of the sensor magnetization on temperature, we deduced that the maximum frozen current with the present setup was $I = 13.5$ mA. This value, much smaller than the expected current $I = 50$ mA, is certainly due to a weaker critical current at a point of the meander. In other meander shape pick-up coils from the same batch, a superconducting current of 50 mA has been frozen [4].

The pulses were recorded using a 16-bit acquisition card with a sampling frequency set at 100 kHz. The data was acquired continuously. By the fact that we want to characterize the detection efficiency curve, all the events have to be counted, including the pile up events. For this reason, the spectrum was obtained using two types of filtering. The first one is a strong differentiator filter which permits to detect pulses and possible pile up events. Knowing each pulse position in the recorded data, we

can determine the energy corresponding to these pulses with a template. The pulses that correspond to events in the sensor are rejected; the discrimination is based on the pulse shape. A spectrum with 740 000 counts acquired during 2.7 days is reported in Fig. 4.

5 Results

At 16 mK, the experimental pulse height per unit of energy is 1 $m\Phi_0$/keV (Fig. 3). The pulses exhibit a 10–90% rise time of 33 μs and a 10–90% decay time of 23 ms. As mentioned above, the current I that magnetized the sensor was much smaller than expected. The consequence on the signal size is significant; with a current of 50 mA we expect a signal size of 2.4 $m\Phi_0$/keV at 16 mK.

The energy resolution (FWHM) is 320 eV at 30 keV and 600 eV at 355.97 keV taking into account a baseline correction. Despite this correction, the energy resolution is linearly dependent on photon energy from 160 keV. With an additional polynomial correction of the pulse amplitude as a function of time, the energy resolution at 355.97 keV is 560 eV.

The measured SQUID flux noise level is 2.2 $\mu\Phi_0/\mathrm{Hz}^{\frac{1}{2}}$ and this is the main contribution to the energy resolution at low energy up to 160 keV. By the two-stage SQUIDs set up, this noise level could be improved by 50%. Therefore by improving the SQUID noise and by freezing a current $I = 50$ mA, an energy resolution below 100 eV could be reached.

We compared the Compton background level of this spectrum with the level measured with a Ge planar geometry detector. The ratio between the 30.97 keV peak area and the Compton level is 1.7 higher with our detector. The linearity of the detector is better than 0.1% from 8.02 keV up to 383.84 keV.

A first characterization of the intrinsic detection efficiency has been done. The peaks were fitted with a Gaussian profile for γ-ray peaks and with a Voigt profile for X-ray peaks. In Fig. 2, the major part of the experimental detection efficiency and the simulated detection efficiency are in good agreement. For 3 of 12 data points

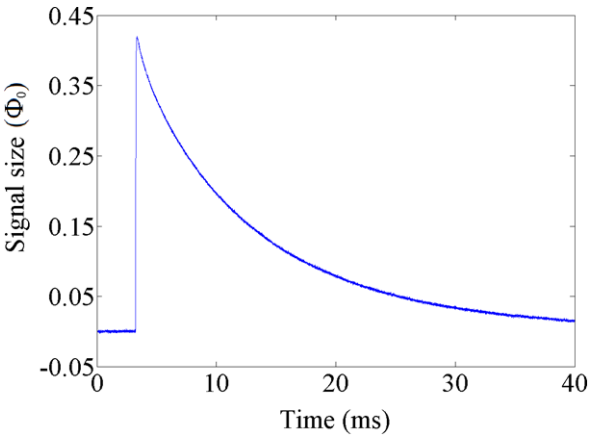

Fig. 3 (Color online) Typical recorded pulse resulting from the absorption of a 383.8 keV photon in the detector at 16 mK with $I = 13.5$ mA

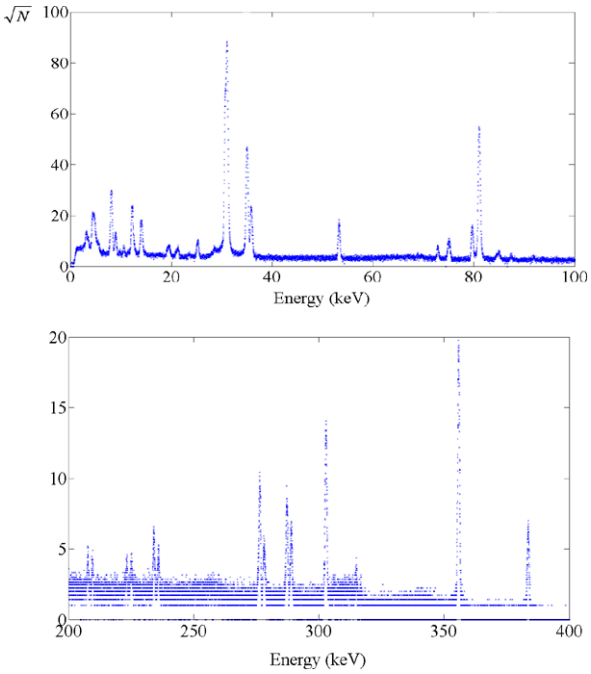

Fig. 4 (Color online) Energy spectra of ^{133}Ba photons in two different energy ranges. The *vertical axis* is the square root of the number of counts per channel

(30 keV, 53 keV and 81 keV) slight discrepancies are observed. These discrepancies could come from systematic errors due to a not perfect peak shaping and an imperfect alignment of the ensemble source-collimator-detector. We will identify these errors and improve the uncertainties on the detection efficiency characterization.

6 Conclusion and Perspective

Despite the fact that the observed pulse heights are lower than expected due to a smaller frozen current, this first γ-ray MMC using a meander shape pick-up coil showed advantageous performances. The linearity and the Compton background level compared with a semiconductor detector are already good. Some improvements have to be done concerning the energy resolution and the determination of the intrinsic detection efficiency. An energy resolution better than 100 eV should be achievable. This energy resolution associated with an improved peak shaping in the energy spectrum will greatly enhance the accuracy on the characterization of the detection efficiency with the energy. This development is promising for accurate determination of X-ray and γ-ray emission probabilities.

References

1. K. Debertin, R.G. Helmer, *Gamma and X-Ray Spectrometry with Semiconductor Detectors* (North-Holland, Amsterdam, 1988)

2. H. Rotzinger, M. Linck, A. Burck, M. Rodrigues, M. Loidl, E. Leblanc, L. Gastaldo, A. Fleischmann, C. Enss, J. Low Temp. Phys. (2008). doi:10.1007/s10909-008-9787-5
3. A. Fleischmann, C. Enss, G. Seidel, in *Cryogenic Particle Detectors*, ed. by C. Enss (Springer, Berlin, 2005), pp. 151–216
4. A. Burck, S. Kempf, H. Rotzinger, M. Rodrigues, L. Gastaldo, A. Fleischmann, C. Enss, J. Low Temp. Phys. (2008). doi:10.1007/s10909-007-9659-4
5. A. Fleischmann, T. Daniyarov, R. Weis, C. Enss, G.M. Seidel, AIP Conf. Proc. **605**, 67–70 (2002)
6. D. Drung, M. Mück, in *The SQUID Handbook*, ed. by C.J. Braginski. Fundamentals and Technology of SQUIDs and SQUID Systems, vol. 1 (Wiley-VCH, New York, 2004), pp. 127–170